Journal of Engineering Science and Technology
Vol. 12, No. 11 (2017) 2896 - 2908

DAM BREACH PARAMETERS AND THEIR INFLUENCE ON FLOOD HYDROGRAPHS FOR MOSUL DAM

TALAL A. BASHEER*, AIMRUN WAYAYOK, BADRONNISA YUSUF, MD ROWSHON KAMAL

Faculty of Engineering, University Putra Malaysia, 43400 UPM Serdang, Selangor, Malaysia
*Department of Dams and Water Resources Engineering, College of Engineering, University of Mosul, Mosul, Iraq
*Corresponding Author: talalbasheer@yahoo.com

Abstract

Dams breach geometry prediction is crucial in dam break studies. The characteristics of flood hydrographs resulting from a dam breach essentially depend on the breach geometry and the required time for breach formation. To investigate the impact of breach parameters on maximum breaching outflows, five breach prediction approaches were implemented to calculate the flood hydrographs using HEC-RAS model, for Mosul dam. Numerous reservoir water levels for each approach were considered. Sensitivity analysis was carried out to evaluate the effect of each parameter on the resulting flood hydrographs. The time and value of peak discharge for each scenario were analysed and discussed. Results show that the most suitable method for estimating breach parameters for Mosul dam was the Froehlich approach. Furthermore, the sensitivity analysis shows that the breach side slope does not affect the peak discharge time and has a minor influence on peak outflow values. Meanwhile, the required time for the breach to develop was highly sensitive to both peak discharge and peak discharge time.

Keywords: Dam break, Mosul dam, Breach, Flood hydrograph, Sensitivity analysis, HEC-RAS.

1. Introduction

Dams provide many benefits to civilisation; however, floods resulting from dam break could lead to tremendous loss of lives and properties. Dam failures can be caused by overtopping of a dam due to insufficient spillway capacity and insufficient free board throughout large inflows to the reservoir, seepage or piping

Nomenclatures

B	Breach width, m
B_{avq}	Average breach width, m
C_b	Reservoir volume coefficient
g	Standard gravitational acceleration, m/s^2
h_b	Breach height, m
h_d	Dam height, m
h_w	Depth of water above the bottom of the breach, m
k_o	Mode of failure coefficient
Q	Discharge, m^3/s
Q_p	Peak discharge, m^3/s
t_f	Breach formation time, hr
T_p	Time of peak discharge, hr
V_{er}	Volume of material eroded from the dam embankment, m^3
V_{out}	Volume of water that passes through the breach, m^3
V_w	Reservoir volume at the time of failure, m^3
z	Breach side slope

Abbreviations

DEM	Digital Elevation Model
HEC-RAS	Hydrologic Engineering Center - River Analysis System

(internal erosion), settlements due to slope slides on the upstream or downstream faces of dam body, liquefaction of earthen dams due to earthquakes and dam foundation failure. Regardless of the reason, almost all failures begin with a breach formation [1].

Dam break study depends on two primary tasks: estimating the breach flood hydrograph and routing this hydrograph downstream of dam site. Essentially the breach flood hydrograph depends on the prediction of breach geometry and breach formation time.

Breach parameter prediction comprises the highest uncertainty of estimating dam break flood [2]. Empirical approaches used to predict breach parameters rely on data obtained from historical dam failures.

Many dam break simulation models require the user to estimate the breach dimensions individually and provide this information as input to the simulation model. Some of the different approaches for breach parameter prediction are explained in Section 2.

2. The Covering Approaches

Dam breach parameters can be obtained from widely used empirical approaches (Fig. 1). These methods are based on statistical analysis of data derived from documented dam failures, which give reasonable predicted values compared to actual observed values [3].

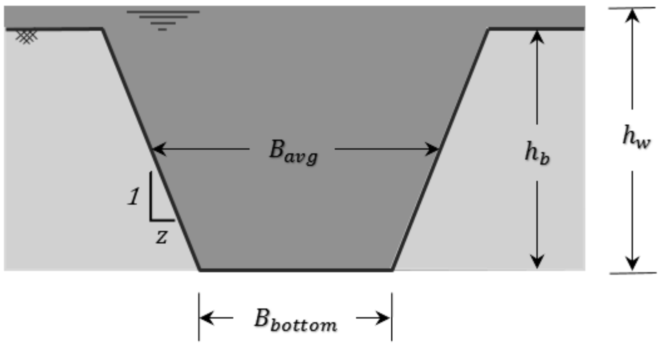

Fig. 1. The breach geometry.

2.1. Singh and Snorrason

Singh and Snorrason [4, 5] presented the early quantitative guidance for breach width prediction. Their study was conducted on data collected from twenty recorded dam failures. Equation (1) shows the breach width limits as a function of dam height. They found that the failure time ranged from 15 minutes to one hour (Eq. (2)).

$$2h_d \leq B \leq 5h_d \tag{1}$$

$$0.25 \leq t_f \leq 1.0 \tag{2}$$

2.2. MacDonald and Langridge-Monopolis

MacDonald and Langridge-Monopolis [6] employed data from forty-two dam failure cases to develop the relationships of the relating breach formation factor, which can be defined as the product of the volume of water that passes through the breach (V_{out}) and water depth in the reservoir at the time of failure, to the volume of material eroded (V_{er}) during the breach.

The researchers indicated that the breach side slopes could be assumed to be 1H:2V in most cases. In addition, an enveloped curve for the breach formation time as a function of V_{er} was also presented for earthfill dams. Equations (3) to (5) represent MacDonald and Langridge-Monopolis equations for V_{er} and breach formation time, as stated by Wahl [7].

Breach width can be calculated from V_{er} and the dam cross section. For earthfill dams:

$$V_{er} = 0.0261(V_{out} * h_w)^{0.769} \tag{3}$$

$$t_f = 0.0179(V_{er})^{0.364} \tag{4}$$

For Non-earthfill dams (earthfill with clay core or rockfill dams):

$$V_{er} = 0.00348(V_{out} * h_w)^{0.852} \tag{5}$$

2.3. Bureau of Reclamation

Bureau of Reclamation (USBR) [8] provided a conservative formula to evaluate the dam breach width with respect to reservoir water depth (Eq. (6)). This formula can be considered as a guideline for choosing the ultimate breach width, which can be employed in hazard classification studies. The recommended breach formation time is 0.011 multiplied by the breach width as shown in Eq. (7).

$$B = 3\ h_w \tag{6}$$

$$t_f = 0.011\ B \tag{7}$$

2.4. Von Thun and Gillette

Von Thun and Gillette [7, 9] used data collected from fifty-seven historic dam failures to develop a relationship for estimating average breach as a function of water depth and a coefficient (C_b) depending on reservoir size, as shown in Eq. (8) and Table 1.

$$B_{avg} = 2.5\ h_w + C_b \tag{8}$$

Table 1. C_b coefficient values with respect to reservoir size.

Reservoir Size (m^3)	C_b (m)
< 1.23∗10^6	6.1
1.23∗10^6 ~ 6.17∗10^6	18.3
6.17∗10^6 ~ 1.23∗10^7	42.7
> 1.23∗10^7	54.9

The authors recommend using breach side slopes of 1H:1V except for dams with cohesive shells or wide cohesive cores, where slopes of 1H:2V to 1H:3V may be more suitable. For the breach development time, Von Thun and Gillette developed two sets of equations depending upon the dam material, shown in Equations (9) to (12).

Breach development time as a function of (h_w):

$$t_f = 0.02\ h_w + 0.25 \qquad \text{(erosion resistance)} \tag{9}$$

$$t_f = 0.015\ h_w \qquad \text{(easily resistance)} \tag{10}$$

Breach development time as a function of (h_w and B_{avg}):

$$t_f = \frac{B_{avg}}{4h_w} \qquad \text{(erosion resistance)} \tag{11}$$

$$t_f = \frac{B_{avg}}{4h_w + 61.0} \qquad \text{(easily resistance)} \tag{12}$$

2.5. Froehlich

One of the recent studies on dam breach is presented by Froehlich [10], which can be considered as a further enhancement of his breach equations by increasing the data sets. Froehlich states that the average side slopes are equal to 1H:1V for overtopping failure and 0.7H:1V for piping and seepage failure.

Froehlich's regression equation for average breach width is presented in Eq. (13):

$$B_{avg} = 0.27\ K_o V_w^{\ 0.32} h_b^{\ 0.04} \tag{13}$$

where, $K_o = 1.0$ for piping, and $K_o = 1.3$ for overtopping failure mode.

The breach development time (Eq. (14)) is related inversely to the breach height and directly to reservoir volume. That means for a given reservoir volume, dams with greater height tend to produce shorter failure times.

$$t_f = 63.2\sqrt{\frac{V_w}{g\ h_b^{\ 2}}} \tag{14}$$

From the available literature on dam breakage and breach prediction methods, one can observe that breach prediction approaches are driven based on documented dam failures for a wide range of dam sizes, mostly small to medium size dams. The main objective of this research is to examine the applicability of these breach prediction methods for Mosul dam. In addition to this, the effect of breach parameters on the resulting flood hydrographs will be studied.

3. Methods

In this study, five of the most common empirical approaches for predicting dam breach size and breach formation time were used to estimate breach parameters for Mosul dam. The employed methods are Singh and Snorrason [4, 5], MacDonald and Langridge-Monopolis [6], Bureau of Reclamation [8], Von Thun and Gillette [7, 9], and Froehlich [10]. These methods were driven from statistical analysis of data extracted from historic dam failures of a wide range of dam sizes. These methods were applied to estimate Mosul dam breach under different scenarios of assumed overtopping and piping failure modes with different ranges of initial reservoir water levels. A range of water levels at 5 m intervals between the maximum reservoir storage level (335 m a.s.l.) to the minimum operating level (300 m a.s.l.) were studied for each method. The breach location was assumed to be at the dam centreline for both overtopping and piping failure modes and the elevation of piping was considered at the level $h_w/2$. The breach final bottom elevation was assumed to be in the main riverbed.

3.1. Study area

Mosul dam was selected to be a case study in this research (Figs. 2 and 3). It is a multi-purpose dam constructed for flood control, irrigation, water supply and hydropower and was put into operation in 1986. Mosul dam is an earthfill dam with a clay core (Fig. 4) located on the Tigris River, which is about 50 km to the north of Mosul city, Iraq. The dam is 3.4 km long, 113 m high, has a 10 m crest width, and the crest elevation is 343 m above sea level. The reservoir capacity is 11.11 km^3 at the maximum operating level (330 m a.s.l.). The dam has a main controlled concrete spillway with five radial gates, located on the left side abutment. The spillway invert level is 330 m a.s.l. The dam has a secondary fuse plug spillway located on the left side of the dam body.

Fig. 2. Location map of the study area.

Fig. 3. Mosul dam satellite view.

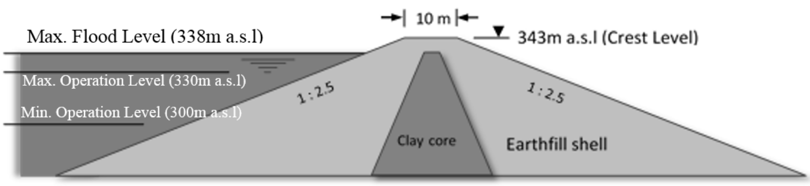

Fig. 4. Schematic diagram of Mosul dam cross section.

3.2. The flood hydrograph

The Hydrologic Engineering Centre's River Analysis System (HEC-RAS Version 4.1.0, 2010) modelling software developed by the U.S. Army Corps of

Engineers was used to determine the flood hydrograph produced by a dam breach for each scenario [11, 12]. Within HEC-RAS, an unsteady flow model was developed for Mosul dam break. The study area was modelled using inline structure to present the dam body, storage area for the reservoir and one dimensional river profile.

Sixteen main cross sections were used to demonstrate the Tigris River reach, extracted from a 30 m × 30 m Digital Elevation Model (DEM). An additional interpolated cross-section with 1000 m intervals was employed, which was generated using HEC-RAS interpolation tool. In total, 89 cross-sections were used in the analysis. The length of Tigris River is about 87.8 km and this value was used in this study.

3.3. Sensitivity analysis

In order to examine each parameter of the breach and breach formation time, a sensitivity analysis was conducted. The sensitivity analysis was performed using the Froehlich method based on overtopping failure mode and maximum operating level at 330 m a.s.l.

The breach width (B_{avg}), side slope (z) and formation time (t_f) were increased by 25%, 50%, 75% and 100% and decreased by 25%, 50% and 75%, respectively and the resulting flood hydrograph at the dam site was estimated for each case.

4. Results and Discussion

The flood hydrograph resulting from Mosul dam breach was calculated using HEC-RAS model for different approaches and under several scenarios, as shown in Tables 2 and 3. Figure 5 shows the flood hydrographs for different reservoir elevations for MacDonald and Langridge-Monopolis approach.

Table 2. Maximum discharge for all scenarios.

	Froehlich		USBR	Singh & Snorrason	Von Thun & Gillette		MacDonald & Monopolis
Reservoir Elev.	Q_p (m^3/s) Overtopping	Q_p (m^3/s) Piping	Q_p (m^3/s) Overtopping	Q_p (m^3/s) Overtopping	Q_p (m^3/s) Overtopping Eq. (9)	Q_p (m^3/s) Overtopping Eq. (11)	Q_p (m^3/s) Overtopping
335	582135	619903	486695	550249	501595	509325	624417
330	554868	544987	413385	471509	433268	443063	563293
325	487058	465882	362989	397736	371576	382650	501661
320	427733	385558	299425	335157	312209	325596	435601
315	3683498	321891	247591	278573	263797	276502	378501
310	313009	266089	206996	229520	227472	229549	313973
305	245877	216560	166442	189291	187790	190695	273431
300	197731	165282	129250	143460	150387	154447	210327

Table 3. Time of maximum discharge for all scenarios.

	Froehlich		USBR	Singh & Snorrason	Von Thun & Gillette		MacDonald & Monopolis
Reservoir Elev.	T_p (hr) Overtopping	T_p (hr) Piping	T_p (hr) Overtopping	T_p (hr) Overtopping	T_p (hr) Overtopping Eq. (9)	Eq. (11)	T_p (hr) Overtopping
335	6.0	6.5	3.0	1.0	2.0	1.0	6.0
330	6.0	6.0	3.0	1.0	2.0	1.0	6.0
325	6.0	6.0	2.5	1.0	2.0	1.0	6.0
320	6.0	6.0	2.5	1.0	2.0	1.0	6.0
315	6.0	5.5	2.5	1.0	2.0	1.0	6.0
310	6.0	5.5	2.0	1.0	1.5	1.0	5.5
305	6.0	5.0	2.0	1.0	1.5	1.0	5.5
300	5.5	5.0	2.0	1.0	1.5	1.0	5.0

4.1. Maximum discharge and time of its occurrence

The results show that there are two sets of flood hydrographs for the same reservoir elevation, as shown in Fig. 6. The first set of flood hydrographs represents those with a small time of breach formation that result in a lower peak discharge and less time of peak discharge. These hydrographs obtained using USBR, Singh & Snorrason and Von Thun & Gillette methods. The most likely causes of lower peak discharge and less time of peak discharge for the first set are the USBR and Singh & Snorrason methods depend on guidance for selecting breach width and breach formation time, in addition to that, these methods were originally obtained from a limited number of dam break cases. While, Von Thun & Gillette method tends to under-predict the breach formation time, which was also observed by Wahl [7]. The second set of flood hydrographs obtained using the Froehlich, for overtopping and piping failure modes and the MacDonald and Langridge-Monopolis methods. These hydrographs provide reasonable values for peak discharge and peak discharge time compared to the first set of hydrographs. The results agree with other studies, such as Wahl [7] and the office of Colorado State Engineer/Dam Safety Branch [3].

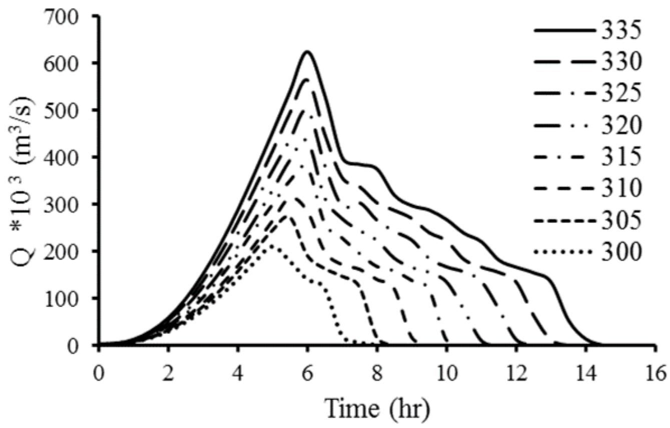

Fig. 5. Flood hydrographs for different reservoir elevations using MacDonald and Langridge-Monopolis approach.

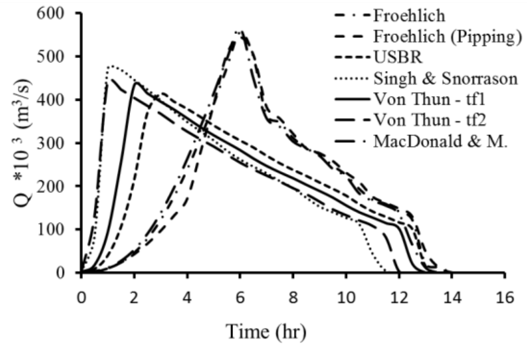

Fig. 6. Flood hydrographs when reservoir elevation is at 330 a.s.l. for all approaches.

4.2. Effect of failure mode

To investigate the effect of dam failure mode, the Froehlich method was used to predict breach geometry for different reservoir elevations using overtopping and piping failure modes. The results show that the overtopping failure mode tends to give higher peak discharge values than the piping failure mode by 1.8 to 19.6% in case of 330 and 300 m a.s.l. reservoir water levels, respectively. This variation in the percentage occurs due to the effect of the hydraulic head on the dam body erosion and time to the full breach formation. The resulting flood hydrographs for both modes are shown in Figs. 7(a) and 7(b).

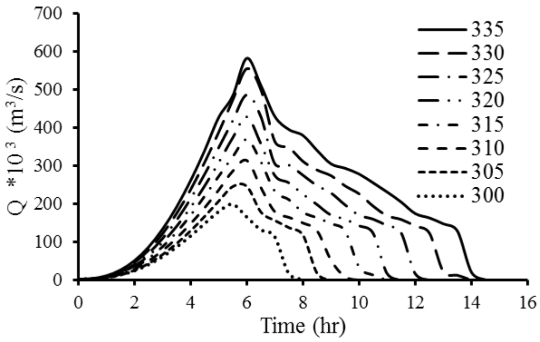

(a) Overtopping

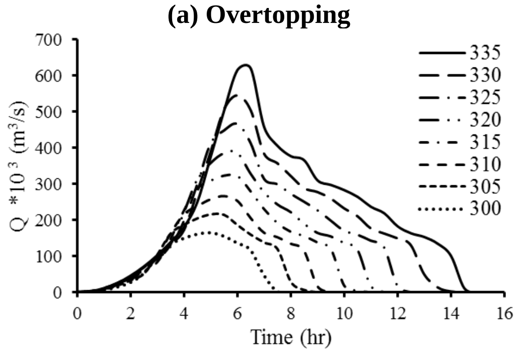

(b) Piping

Fig. 7. Flood hydrographs for different reservoir elevations using Froehlich approach.

4.3. Sensitivity analysis

Breach width, side slope and formation time were analysed to determine the controlling parameter of peak discharge (Q_p) and time of peak discharge (T_p).

4.3.1. Breach width

The sensitivity analysis results show that increasing the breach width by a constant percentage leads to a slight increase in the Q_p but a decrease in the T_p and vice versa. For instance, decreasing breach width by 50% increases the Q_p by 12.1% and decreases T_p by 8.33%, as shown in Figs. 8 and 9.

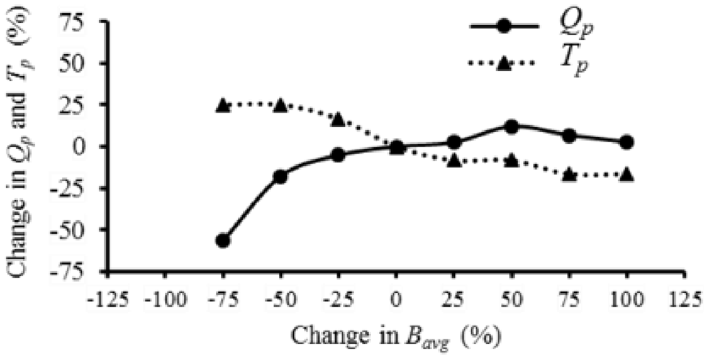

Fig. 8. Percent change in Q_p and T_p with B_{avg}.

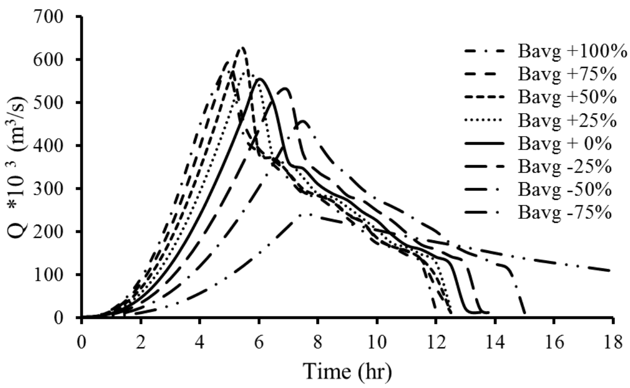

Fig. 9. Flood hydrographs for different B_{avg} values at dam site.

4.3.2. Side slope

From the results obtained from this study, no change was noticed in peak discharge time with changes in breach side slopes. However, changing breach side slope leads to a slight change in breach cross-section area. Therefore, the effect of breach side slope in the case of Mosul dam can be negligible, as shown in Figs. 10 and 11.

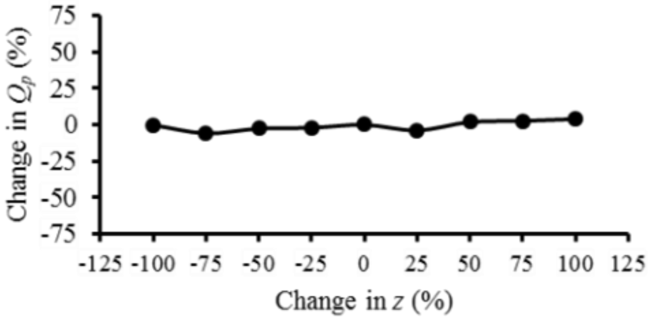

Fig. 10. Percent change in Q_p with breach side slope.

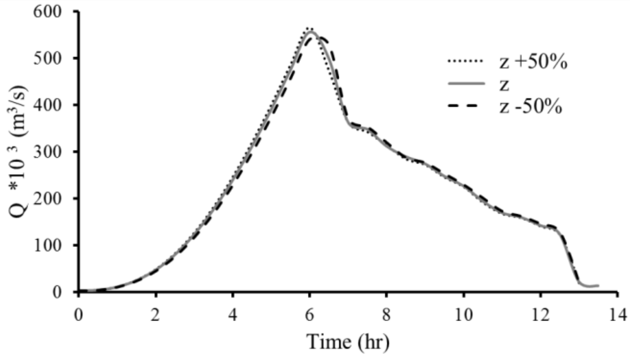

Fig. 11. Flood hydrographs for different *z* values at the dam site.

4.3.3. Breach formation time

The results specify that the Q_p and T_p were highly sensitive to changes in breach formation time. From Table 4 and Figs. 12 and 13, increasing breach formation time by 50% lead to decreasing Q_p by 19.19% and increasing T_p from 6 hr to 9.5 hr (i.e., 58.33% increase). At the same time, reducing breach formation time by 50% led to increasing Q_p by 39.3% and decreasing T_p from 6 hr to 3.5 hr (i.e., 41.67% decrease). The sensitivity analysis outcome for breach formation time agrees with others dam breach studies, such as Fread [13] and Froehlich [14].

Table 4. Values of changed time of breach formation, maximum discharge and time of maximum discharge.

t_f hr	t_f dif. %	Q_p m^3/sec	Q_p dif. %	T_p hr	T_p dif. %	Note
14.856	+100	374593	-32.49	11.5	91.67	Increased t_f
12.999	+75	423784	-23.62	10.5	75	
11.514	+50	448369	-19.19	9.5	58.33	
9.285	+25	489175	-11.84	7.5	25	
7.428	0	554868	0	6	0	Original t_f
5.571	-25	604355	8.92	4.5	-25	Decreased t_f
3.714	-50	772942	39.3	3.5	-41.67	
1.857	-75	866670	56.19	2	-66.67	

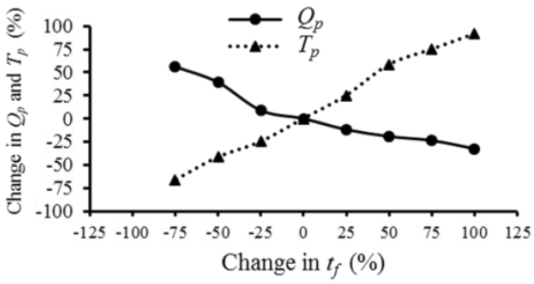

Fig. 12. Percent change in Q_p and T_p with t_f.

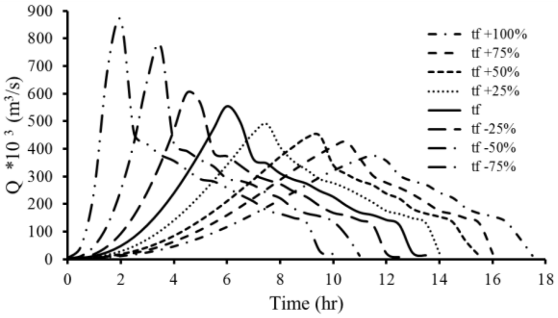

Fig. 13. Flood hydrographs for different t_f at the dam site.

To sum up, the sensitivity analysis results show that breach side slope didn't change the peak discharge time and had only a slight effect on peak discharge values. In other words, the outflow hydrograph is not sensitive to the breach side slope, while the outflow hydrograph is adequately sensitive to the breach width. The most effective parameter was the breach formation time (i.e., the outflow hydrograph is highly sensitive to the breach formation time).

5. Conclusions

Flood hydrographs resulting from a dam breach are studied by applying five of the common breach prediction approaches to Mosul dam. Different scenarios were applied to cover overtopping and piping failure modes. In addition, eight reservoir levels were considered for each approach. Some concluding remarks from the study are given below:

- USBR, Singh & Snorrason and Von Thun & Gillette methods under-predicted the average breach width and the breach formation, which resulted in a sharp flood hydrograph with lower peak discharge and time of peak discharge.
- Froehlich and MacDonald & Langridge-Monopolis methods give reasonable values for peak discharge and time of peak discharge compared to the other methods.
- Overtopping mode of failure tends to provide sharper and higher peak discharge compared to piping failure mode.

- The sensitivity analysis shows that the peak discharge and peak discharge time is less sensitive to breach width but highly sensitive to breach formation time. Meanwhile, the breach side slope has a negligible effect on peak discharge and no effect on peak discharge time.

References

1. Xiong, Y. (2011). A dam break analysis using HEC-RAS. *Journal of Water Resource and Protection*, 3(6), 370-379.
2. Wurbs, R.A. (1987). Dam-breach flood wave models. *Journal of Hydraulic Engineering*, 113(1), 29-46.
3. Colorado Dam Safety Branch (2010). Guidelines for dam breach analysis. Department of Natural Resources, Division of Water Resources, Colorado. Retrieved March 20, 2017, from http://water.state.co.us/DWRDocs/Policy/ Pages/DamSafetyPolicies.aspx
4. Singh, K.P.; and Snorrason, A. (1982). Sensitivity of outflow peaks and flood stages to the selection of dam breach parameters and simulation models. *SWS Contract Report 289*, State Water Survey Division, Surface Water Section, Illinois. Retrieved March 20, 2017, from http://www.isws.illinois.edu
5. Singh, K.P.; and Snorrason, A. (1984). Sensitivity of outflow peaks and flood stages to the selection of dam breach parameters and simulation models. *Journal of hydrology*, 68(1-4), 295-310.
6. MacDonald, T.C.; and Langridge-Monopolis, J. (1984). Breaching characteristics of dam failures. *Journal of Hydraulic Engineering*, 110(5), 567-586.
7. Wahl, T.L. (1998). Prediction of embankment dam breach parameters – a literature review and needs assessment. *Dam Safety Report DSO-98-004*, U.S. Bureau of Reclamation. Retrieved March 20, 2017, from https://www. usbr.gov
8. U.S. Bureau of Reclamation (1988). Downstream hazard classification guidelines. ACER Technical Memorandum No. 11, U.S. Bureau of Reclamation, Denver, Colorado. Retrieved March 20, 2017, from https:// www.arcc.osmre.gov
9. Von Thun, J.L.; and Gillette, D.R. (1990). Guidance on breach parameters. *unpublished internal document*, U.S. Bureau of Reclamation, Denver, Colorado.
10. Froehlich, D.C. (2008). Embankment dam breach parameters and their uncertainties. *Journal of Hydraulic Engineering*, 134(12), 1708-1721.
11. USACE (2010). HEC-RAS hydraulic reference manual. Version 4.1, U.S. Army Corps of Engineers, Hydrologic Engineering Center.
12. USACE (2014). Using HEC-RAS for dam break studies. *Report No. TD-39*. U.S. Army Corps of Engineers, Hydrologic Engineering Center. Retrieved March 20, 2017, from http://www.hec.usace.army.mil/publications
13. Fread, D.L. (1988). Breach: An erosion model for earthen dam failures. National Weather Service, National Oceanic and Atmospheric Administration, Silver Springs, Maryland. Retrieved March 20, 2017, from http://www.nws.noaa. gov/ohd/hrl/hsmb/docs/hydraulics/papers_before_2009/hl_209.pdf
14. Froehlich, D.C. (1987). Embankment-dam breach parameters. *In Hydraulic Engineering, Proceedings of the 1987 National Conference.* Williamsburg, VA, USA, 570-575.